3. N. I. Akatnov, "Dual-scale semiempirical theory of turbulent boundary layers and streams," Izv. Akad. Nauk SSSR, Mekh. Zhidk. Gaza, No. 6 (1982).
4. S. A. Losev, Hydrodynamic Lasers [in Russian], Nauka, Moscow (1977).
5. S. V. Kulikov, "Comparison of the calculations for the power of a CO_2 HDL made under different steady-state generation conditions," Zh. Prikl. Mekh. Tekh. Fiz., No. 2 (1980).
6. P. Kassadi, J. Newton, and P. Rouz, "A new type of mixing hydrodynamic laser," Raket. Tekh. Kosmon., 16, No. 4 (1978).
7. V. A. Pivovar, "Limited application for an approximation of the vibrational temperature for nitrogen in a short pulse duration CO_2–N_2–He laser," Zh. Tekh. Fiz., 47, No. 2 (1977).
8. B. V. Egorov and V. N. Komarov, "A comparative analysis of the kinetic models for vibrational relaxation in mixtures of gases containing CO_2," ChMMSS, 11, No. 3 (1980).
9. E. T. Antropov, V. T. Karpukhin, and Yu. B. Konev, "A theoretical investigation of the characteristics of high temperature hydrodynamic lasers," Preprint Institute of HIgh Temperatures, Akad. Nauk SSSR, Nos. 5-37 (1979).
10. T. A. Bungova, A. V. Lavrov, T. A. Spas, and S. S. Kharchenko, "Nonequilibrium physical and chemical processes in a system of two-dimensional turbulent, undesigned streams," in: Stream Flows of Liquids and Gases [in Russian], Novopolotsk (1982).
11. B. V. Abakumov, Yu. V. Kurochkin, et al., "A hydrodynamic laser with thermally nonequilibrium electric-arc heating," Kvantovaya Elektron., No. 9 (1979).

CALCULATION OF NON-STEADY-STATE FLOWS OF RELAXED GASES IN CHANNELS

A. V. Chirikhin

UDC 532.542+532.54/55.011.55

Maintaining control at supersonic velocities in the atmosphere requires experimental investigations of flow around aircraft for a wide range of Mach and Reynolds numbers. One technique for modeling such flow involves the use of a high-enthalpy wind tunnel. Examples of such set-ups include pulse-driven tunnels with gas heated by a discharge in a confined volume [1] and tunnels with electric-arc heaters [2]. In the first case all of the working processes are non-steady-state, and in the second case one begins with non-steady-state output where the established flow is in the ripple state. It is natural to assume that in the given cases the nonlinear interaction of wave structures has a significant effect on the formation of the flow of a real gas. Such an interaction arises when the diaphragm in a tunnel breaks down and when the energy input is periodic. Of particular importance are the problems in [3], which are related to pulsed heating of the CO_2 flow by an electrical discharge with a small duration. It was shown in [4] that the modified technique of S. K. Godunov is an effective way for studying similar flows. In this study Godunov's technique relating to flows with external energy input [4] is applied for calculations of flows with vibrational relaxation. This technique is shown to be useful for numerical modeling of steady-state flows in nozzles, non-steady-state flows in pulse-driven wind tunnels, and for flows with periodic energy input into the subsonic zone of a channel, which reproduces the flowing part of a coaxial heater and a supersonic nozzle of a typical high-enthalpy wind tunnel. Questions regarding similarity and the modeling of non-steady-state flows with vibrational relaxation are considered.

1. Nonequilibrium energy exchange between vibrational and active degrees of freedom for molecules (the V–T process) reflects the basic behavior of relaxation phenomena and allows one to easily model the effect of relaxation on the flow of a high temperature gas. On the other hand, such a calculation technique can be used for solving a variety of problems related to nonequilibrium flow of carbon dioxide and carbon dioxide mixtures [5].

Zhukovskii. Translated from Zhurnal Prikladnoi Mekhaniki i Tekhnicheskoi Fiziki, No. 6, pp. 87-95, November-December, 1985. Original article submitted July 20, 1984.

 0021-8944/85/2606-0836$09.50 © 1986 Plenum Publishing Corporation

We will consider quasi-one-dimensional non-steady-state flow of a nonviscous, nonthermally conducting gas in a channel of variable cross section taking into account vibrational relaxation. We will assume that in some part of the channel the energy of vibration can play the role of a parameter. Such an approach allows one to consider vibration as a source (a discharge) of energy and the V–T process as a means of external energy exchange whose description is given by the Landau–Teller model. The corresponding system of dimensionless equations for the relaxation dynamics of the gas have the form

$$\mathrm{Sh}\, f\frac{\partial \rho}{\partial t}+\frac{\partial \rho u f}{\partial x}=0,\ \mathrm{Sh}\,\rho\frac{\partial u}{\partial t}+\rho u\frac{\partial u}{\partial x}+\frac{\partial p}{\partial x}=0,$$

$$\frac{\varkappa}{\varkappa-1}\left(\mathrm{Sh}\,\rho\frac{\partial T}{\partial t}+\rho u\frac{\partial T}{\partial x}\right)-\mathrm{Sh}\frac{\partial p}{\partial t}-u\frac{\partial p}{\partial x}=\mathrm{Sh}\,\rho q,$$

$$\mathrm{Sh}\frac{\partial e}{\partial t}+u\frac{\partial e}{\partial x}=\mathrm{Sh}\,q,\ q=\frac{e(T_i)-e(T)}{\tau_i(p,\ T)},$$

$$f(x)=\frac{F}{F^0},\ p=\rho T,\ e(T)=I_1\left[\exp\left(\frac{I_1}{T}\right)-1\right]^{-1},$$

$$\tau_i(p,\ T)=\frac{I_2}{p}\exp\left[I_3\left(\frac{I_1}{T}\right)^{\frac{1}{3}}\right]; \tag{1.1}$$

$$\mathrm{Sh}=\frac{l}{t^0(RT^0)^{1/2}},\ I_1=\frac{\Theta}{T^0},\ I_2=\frac{A}{t^0p^0},\ I_3=\frac{B}{\Theta^{1/3}}. \tag{1.2}$$

Here ρ is the density; p, pressure; u, velocity; T, T_i, statistical and vibrational temperatures, respectively; e(T), $e(T_i)$, vibrational energies; t, time; τ_i, time for vibrational relaxation; f and F, areas of the flow filaments; x, position; R, gas constant; κ, adiabatic freezing exponent; θ, characteristic temperature of the vibrations; A and B, constants in the equation for the relaxation time $\tau_i = (A/p)\exp(BT^{-1/3})$; ; ℓ, characteristic longitudinal scale; Sh, analog to the Strouhal number; I_{1-3}, parameters; and the zero indices denote the characteristic gauges of the corresponding variables. Hence, the density is referenced to p^0/RT^0, the velocity to $(RT^0)^{1/2}$, the energy to RT^0, and the position to ℓ.

We will use the initial values of p and T for some initial cross section F^0 as their gauges, and the quantity of this cross section will be used as a gauge for the area of the flow filament. Then, for the initial cross section p = T = f = 1.

We will assume that in the channels with equivalent dependences for f(x) the initial distributions of the dimensionless functions p(x), T(x), and u(x) are reproduced. In the given case the dimensionless distribution of the vibrational energy e(x) and the parameters in (1.2) remain free parameters, which will determine non-steady-state flow with vibrational relaxation. It is easy to see that for a real gas the conditions for reproducing the parameters in (1.2) require the duplication of the initial distributions of the dimensional values for the vibrational energy, the velocity, the statistical temperature, and the parameters

$$\vartheta=t^0p^0,\ \xi=l/t^0. \tag{1.3}$$

Therefore, the characteristic gas dynamics gauge ℓ should be selected from the real conditions of flow, and the product of the parameters ϑ and ξ give still another similarity parameter $L = \ell p^0$.

It would be interesting to model flows with vibrational relaxation using different gases. The adiabatic freezing exponent and the parameter κ play specific roles in this case. One can then establish a correspondence between the flows of the different gases with the conditions of reproducibility for κ and I_3 on the basis of (1.2), where one of the gauge parameters, p^0, t^0, or ℓ, is permitted to vary freely.

In particular, the calculations in [6, 7] allow for steady-state flows of diatomic gases in hyperbolic Laval nozzles. These calculations were made using the interpolation equation of Finni [8] for the relaxation time.

2. The principles behind devising a difference scheme for integrating system (1.1) using the Godunov method is well known [4, 5, 9]. The equations for the conservation of the flow rate and for the quantity of flow are identical to the equations for an ideal gas. Therefore, we will use a difference approximation only for the equations of energy and vibrational relaxation

$$\frac{1}{\varkappa-1}(\rho T)^{m+1/2}=\rho_{m+1/2}\left(\frac{1}{\varkappa-1}T+\frac{u^2}{2}\right)_{m+1/2}-\frac{2\tau}{\Delta x\,(f_m+f_{m+1})}\left[\left\{\rho uf\left(\frac{\varkappa}{\varkappa-1}T+\frac{u^2}{2}\right)\right\}_{m+1}-\left\{\rho uf\left(\frac{\varkappa}{\varkappa-1}T+\frac{u^2}{2}\right)\right\}_m\right]+$$

$$+\frac{\tau}{2}\left[(\rho q)^{m+1/2}+(\rho q)_{m+1/2}\right]-\left(\rho\frac{u^2}{2}\right)^{m+1/2},\qquad(2.1)$$

$$(\rho e)^{m+1/2}=\rho_{m+1/2}\left(e-\frac{\tau}{2}q\right)_{m+1/2}-\frac{2\tau}{\Delta x\,(f_m+f_{m+1})}\left[(\rho ufe)_{m+1}-(\rho ufe)_m\right]-\frac{\tau}{2}(\rho q)^{m+1/2}.$$

Here, τ is an integration step in time, and the remaining definitions are conventional (e.g., see [4]).

Equations (2.1), which are supplemented by the corresponding approximations for the equations of the flow rate and the quantity of flow, are the basis for a numerical algorithm with the condition that one can correctly determine the values of these parameters on the boundaries of the cells. These parameters are determined from the solution of the problem regarding an arbitrary breakdown. A similar approach can be used for the flow of a relaxing gas if the integration step in time τ is chosen taking into account the freezing conditions for the relaxation processes in shock waves [4]. Since for flows with vibrational relaxation the adiabatic freezing exponent is constant over the entire field of the flow, the technique in [9] can be directly applied for calculating the breakdown in this case.

The algorithms mentioned above was tested by making calculations of steady-state, nonequilibrium flow of nitrogen. The calculations were made for a flat nozzle, where the length of the supersonic section was six times greater than the length of the subsonic section. The profiles of the subsonic and supersonic sections were hyperbolic, which were mated to regions of constant cross section with cubical parabolas, where $f/f_* = 5$ at the input and $f/f_* = 10$ at the output of the nozzle. The channel was uniformly subdivided along the longitudinal coordinate, and the total number of spacings was between 100 and 400. The geometric parameters of the nozzle and the stagnation parameters p_0, T_0 were assigned in such a way that $k = 4.7$ from [7], and the results were compared with calculations ($k = h_*/2\tau_i(p_0, T_0)\,\mathrm{tg}\,\varphi(2RT_0)^{1/2}$, where h_* is the height of the critical cross section, and 2φ is the angle between the asymptotes of the hyperbola).

The initial distributions of the gas dynamic functions correspond to the flow of an ideal gas with $\kappa = 1.4$, where the temperature of the vibrations is initially equal to the local statistical temperature. The boundary conditions at the input and output of the channel were formulated according to [4] taking into account flows with nonequilibrium condensation. The integration step in time τ is chosen from the Kurant condition along with the condition

$$\tau < 0.3\tau_i,\qquad(2.2)$$

which ensures that the iterations converge for all the considered variants.

For all calculations $\theta = 3340$ K, and the relaxation time was determined using the Finni equation [8]. In Fig. 1, lines 1 represent the distributions of the statistical T, and lines 2 show the vibrational temperature T_i. The solid lines correspond to calculations with 200 points, and the dashed lines are for calculations with 100 points of subdivision of the nozzle. The calculations with 400 points cannot be distinguished from the distributions indicated with the solid lines. The crosses denote the results from [7] obtained using a second-order cruising approximation. A comparison of the results shows that the calculations are sufficiently accurate even for 100 points of subdivision.

When there exists an extended zone of near-equilibrium flow, condition (2.2) increases the time required for finding a solution. Nevertheless, the time can be reduced almost to the time required for finding the solution for an ideal gas. In this case, it is necessary to divide the flow field into zones of equilibrium and nonequilibrium flow using the Finni criteria for the freezing point of the vibrations

$$de/dt = \alpha e/\tau_i.$$

For $\alpha \lesssim 0.01$ the combined solution differs little from the results of direct calculation and can be obtained after 700-1000 steps in time.

3. We will consider the formation of non-steady-state, nonequilibrium flow of nitrogen which begins after the breakdown of a diaphragm in an axisymmetric channel simulated by a

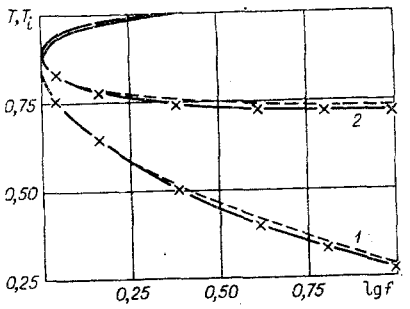

Fig. 1

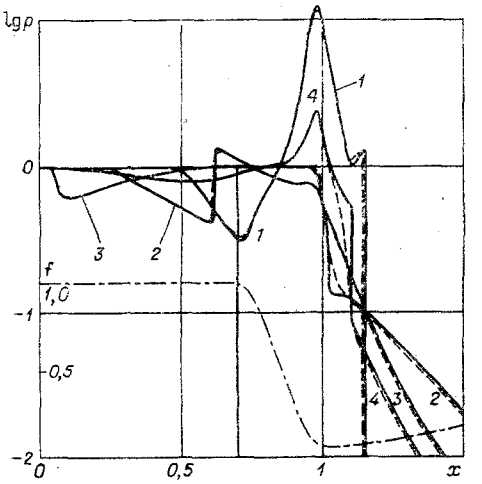

Fig. 2

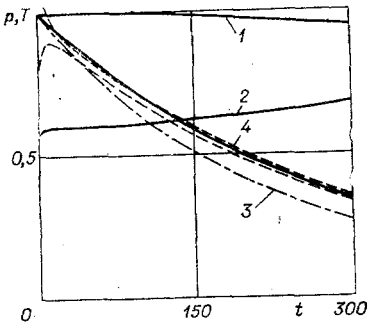

Fig. 3

discharge chamber and the supersonic nozzle of a pulse-driven wind tunnel [1]. This phase of flow precedes the asymptotic state studied in [10, 11] in the approximation of a thermodynamically ideal gas, including the stage when the nozzle is activated [12, 13].

The channel for which the calculations were conducted is represented in Fig. 2 by the dot–dash line. The form of the discharge chamber was that of a cubical parabola, and the supersonic nozzle had the shape of a hyperbola. The linear gauge ℓ was selected to be the distance from the left wall to the critical cross section of the nozzle. The subdivision spacing of the channel for the individual calculation variants was $(1–0.25)\cdot 10^{-2}\ell$, and the total number of steps in the x-direction was between 150 and 600. The diaphragm was positioned at the front of the channel. The pressure ratio at the diaphragm was initially equal to 100, where the statistical parameters in the zone of high pressure corresponded to the equilibrium state for T^0 = 3000 K, and in the zone of low pressure they corresponded to the equilibrium state for T = 300°K.

After breakdown of the diaphragm, a low pressure wave was propagated to the left, and a shock wave, whose intensity increases along the channel, was propagated to the right. The intensity of the shock wave was maximum near the critical cross section. This state is shown by curve 1 in Fig. 2, where the shock wave can be seen to pass through the critical cross section. Then, a compression wave reflects from the critical cross section (curve 2), and a reverse flow is created behind it. Upon reflection from the wall of the discharge chamber (curve 3), the shock wave returns to the region of the critical cross section (curve 4). This cycle is repeated successively. Curves 1-4 correspond to the moments in time 0.1, 0.24, 0.6, and 1.1 for the period of the cycle from the beginning of the flow formation, and the solid and dashed lines represent 600 and 300 subdivision points of the channel, respectively, where the number of points in the supersonic section of the nozzle corresponds to subdivisions of 200 and 100 points (see section 2).

A comparison between the calculation results for different quantities of points and the data of section 2 allows one to conclude that about 600 points are sufficient for calculating the state of the gas in the discharge chamber and the flow of the gas in the nozzle after activation. Therefore, the distributions of the statistical and vibrational temperatures in the nozzle are similar to those represented in Fig. 1.

The calculations show that the period of the vibrational processes in the discharge chamber t^0 is equal to the ratio of the duplication gauge ℓ to the equilibrium velocity of sound a_e, which in our case corresponds to the duplicated value of the parameter $\xi = 0.54 \cdot 10^3$ m/sec ($\vartheta = 0.37 \cdot 10^4$ Pa/sec, $L = 2 \cdot 10^6$ m·Pa).

The vibrational state of the gas in the discharge chamber is combined with a monotonic decrease in pressure due to the discharge of gas in the nozzle for a comparatively small change in the temperature. In Fig. 3 line 1 shows the change in the average temperature of the gas in the discharge chamber T_0, line 2 indicates the change in the ratio of the vibrational freezing temperature T_i to T_0, the dashed lines show the change in the maximum and minimum values of the pressure at the diaphragm as a function of the dimensionless time $t = t/t^0$, and line 3 represents the pressure as a function of the time calculated with Eq. (12) from [10] for a quasi-steady-state discharge when the gas is in an isentropic state. Line 4 gives the dependence

$$p = p^0 \exp\left(-\frac{a_* F_*}{V}\frac{T^0 p_*}{T_* p^0} t\right), \tag{3.1}$$

which is easy to obtain assuming that the gas is in an isothermic state within the discharge chamber and the discharge is quasi-steady-state. In relation (3.1) a_* is the critical velocity of sound, and V is the volume of the discharge chamber. For making the calculation of curves 3 and 4 we have included the data for the steady-state equilibrium discharge of nitrogen at $T_0 = 3000$ K. A comparison of curves 3 and 4 with the dashed lines indicates that the pressure drop in the discharge chamber is practically isothermic. Hence, the degree of nonequilibrium for the flow increases with time. One must take into account the effects of acoustic vibrations from the discharge chamber on the flow for solving some of the problems associated with modeling.

4. We will consider the formation of flow due to the periodic input of energy into the flow filament, whose distribution f(x) models the flowing part of the coaxial heater and the supersonic nozzle. We will assume that the chamber of the heater expands in size from the left and smoothly transfers to the receiving chamber, whose volume substantially exceeds the volume of the heater and the nozzle. When the flow begins to develop in the nozzle, the operation of the heater has a weak effect on the state of the gas in the receiving chamber, and the output compression waves will be greatly attenuated because of the increasing size of the channel. Hence, for the left boundary of the flow field one can use the conditions of constant entropy and complete enthalpy for the influx of gas and can correctly state the boundary conditions (1.122-1.124) from [4].

The profile for the flow filament, where the indicated conditions are sufficiently satisfied, is shown in Fig. 4 with a dot–dash line. The transonic part of this filament is the same as that of section 3. The channel is uniformly subdivided along the x-coordinate. The total number of points is 500, which ensures the necessary accuracy in making calculations.

The energy intake zone is situated at the cross section x = 60, occupying two cells of the channel subdivisions along the x axis, and its length was used as a linear gauge of the flow. The plots are represented taking into account the conditions of similarity (1.3). In particular, the vibrational and statistical temperatures are referenced with the temperature of the cold gas $T^0 = 300$ K.

The values for the parameters in the zone of energy intake were formulated in the following manner. Beginnng with some moment in time t_1 after the flow of the cold gas is established for t, which satisfies the inequality $t - t_1 - (n-1)t^0 \leq \Delta$, $n = 1, 2, 3...$, one assumes that $e = e(T_1)$, $T = T_2$ for $T < T_2$; for $T \geq T_2$ the statistical temperature did not change, $p = \rho T$ (ρ = const). Here, t^0 is the time between the individual pulses, Δ is the duration of the pulse, and $T_{1,2}$ are the vibrational and statistical temperature in the energy input zone. For $T_1 = T_2$ we have an approximation for equilibrium energy input; for $T_1 \neq T_2$ the energy input is in the general case not be in equilibrium. For $\Delta < t^0$ the energy input is periodic, and for $\Delta = t^0$ it is steady-state. In making calculations $\Delta = 0.2t^0$.

The initial distributions for the gas dynamic parameters were obtained by establishing the solution for the flow of cold gas, which was accomplished through the "breakdown" of the diaphragm on the right boundary of the nozzle. Then, the energy input was "turned on". The development of non-steady-state flow through periodic energy input with $T_1 = T_2 = 10$, $\xi = 4$ m/sec, $L = 5 \cdot 10^3$ m·Pa is shown in Figs. 4 and 5. In Fig. 4 the solid lines indicate the

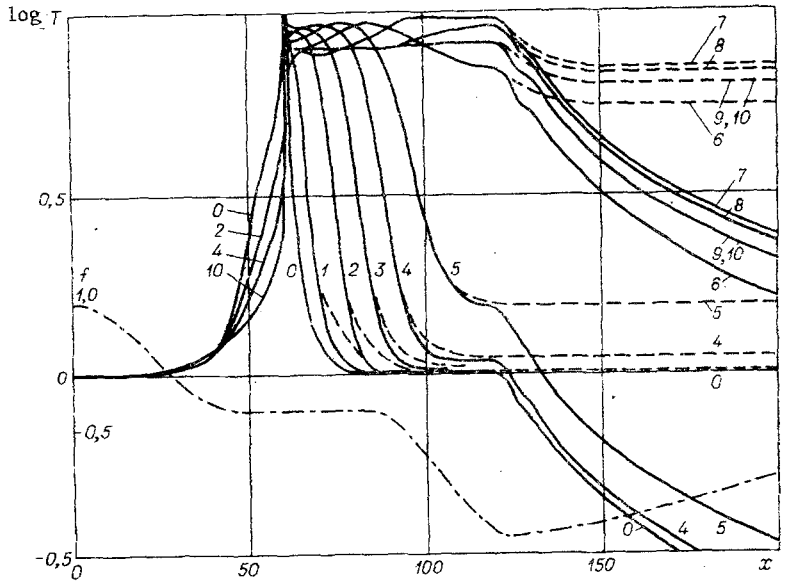

Fig. 4

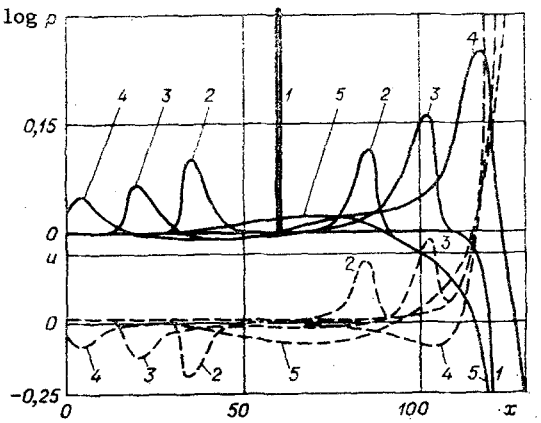

Fig. 5

distributions of the statistical temperature T, and the solid lines show the vibrational temperature T_i. In Fig. 5 the solid lines correspond to the distributions for log p, and the dashed lines are for the velocity distributions u.

When the energy input is "turned" on the temperature of the gas changes abruptly from T^0 to T_1. For ρ = const this leads to a sharp increase in the pressure, where the pressure peak goes beyond the scale of Fig. 5. On the left and the right of the zone of energy input compression waves begin to propagate, and inside this zone a low density wave moves.

Successive positions of the compression waves between the first and second pulses of the energy input are shown by curves 1-5 in the upper part of Fig. 5, and the corresponding velocity distributions are represented in the lower part. The data shows that the gas initially flows to both sides of the energy input zone. The left wave is attenuated because of the low density wave which overtakes it and the expanding form of the channel. The intensity of the right compression wave increases because of the predominating effect of the channel's form. It is then reflected from the critical cross section, and at the beginning of the second pulse a significant part of the subsonic section of the channel is occupied by a region of reverse flow. Such a state greatly increases the intensity of the left compression wave after the secondary energy input and determines the first stage in the formation of the flow when the heated gas flows to the left of the energy input zone.

The maximum shift of the hot "plug" to the left occurs at approximately the end of the tenth pulse and is shown by curve 0 in Fig. 4. Here, the curves with increasing numbers correspond to steps in time of 10 t^0. Curves 1-4 represent the second stage in the formation of the flow when the remainder of the cold gas flows out, and the plug of the initially heated

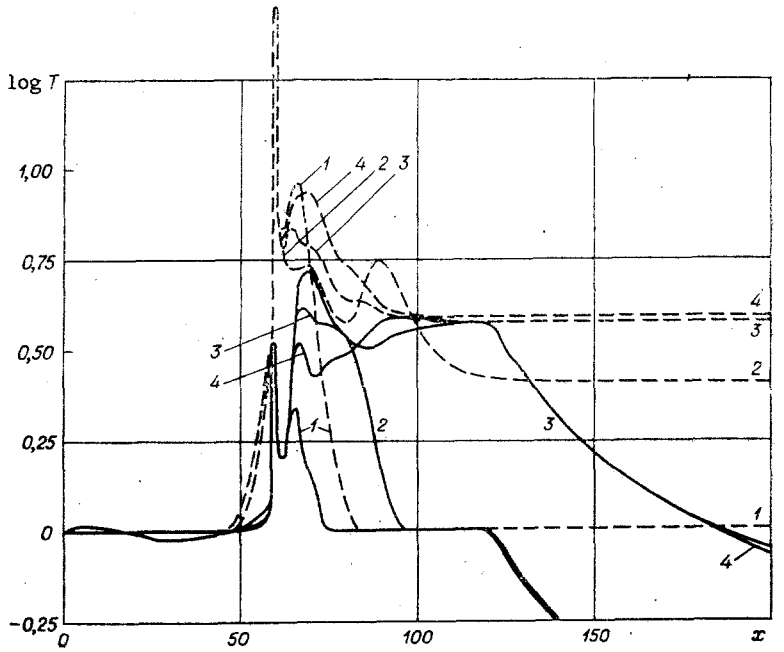

Fig. 6

gas begins to flow to the right. During the third stage (curves 5-7) this plug passes the the critical cross section of the nozzle, and in the energy input zone it comes into contact with the cold gas. In the final stage (curves 8-10) the remainder of the initially heated gas exits the nozzle, and a weakly rippled flow is established. The obtained results conform with the given representation of the basic features of transfer processes in the heaters [14, 15].

It is evident that the approximation used for the equilibrium energy input has some limitations. One can use a general approach for determining these limitations if it is assumed that the statistical and vibrational temperatures in the energy input zone are equal to one another. An example of such calculations is shown in Fig. 6, where the transfer stage is indicated for the parameters $T_1 = 28$, $T_2 = 3.3$, $\xi = 0.4$ m/sec, $L = 50$ m·Pa. In the given case, the transfer of energy during the process of V–T exchange is complicated because of the small value of L, and, on the whole, nonequilibrium flow occurs.

Parametric calculations done in the approximation of both equilibrium and nonequilibrium energy input for different parameters allow one to make the following conclusions: 1) for $L \gtrsim 5 \cdot 10^2$ m·Pa the flow in the heater is nearly in equilibrium, and for $L \lesssim 50$ m·Pa it is typically in nonequilibrium; 2) for equilibrium flow in the heater the transfer processes are basically determined by the position of the energy input zone, and for $\xi \gtrsim 4$ m/sec they weakly depend on the frequency of the energy input; 3) the times for the transfer processes increase with an increase in the nonequilibrium condition of the flow in the heater (for $L < 5 \cdot 10^2$ m·Pa); 4) the final state of the flow is a weak function of the frequency of the energy input for $L > 5 \cdot 10^4$ m·Pa, $\xi > 12$ m/sec.

One should note in conclusion that direct numerical inspection of the role of the similarity parameters from (1.3) in the example of reproducing both the ripple state of the flow in a pulse-driven wind tunnel and the transfer processes with periodic energy input has revealed the specific values of these parameters. In addition, the calculation results were applied to flows of different diatomic gases, where the relaxation time for the vibrations conformed to the interpolation equation of Finni [8].

The author thanks A. N. Kraiko and V. L. Grigorenko for useful discussions on the work.

LITERATURE CITED

1. A. S. Korolev, "Obtaining and studying supersonic flows of carbon dioxide in pulse-driven wind tunnels," Transactions from the N. Ye. Zhukovskii Central Institute of Aerohydrodynamics (TsAGI), No. 1943 (1975).
2. I. I. Mezhirov et al. (eds.) "An experimental set-up for studying the aerodynamics and strength of aircraft," Transactions from the N. Ye. Zhukovskii Central Institute of Aerohydrodynamics (TsAGI), No. 1949 (1979).

3. B. N. Srivastava, Ch. J. Nait, and O. Tsappa, "Suppression of acoustic disturbances in a pulsed laser system," Raket. Tekh. Kosmn., 18, No. 6 (1980).
4. T. A. Saltanov, Nonequilibrium and Non-Steady-State Processes in Gas Dynamics [in Russian], Nauka, Moscow (1979).
5. V. A. Levin and Yu. V. Tunik, "The flow of a relaxing mixture of gases in two-dimensional flat nozzles," Izv. Akad. Nauk SSSR, Mekh. Zhidk. Gaza, No. 1 (1976).
6. G. N. Sayapin, "Nonequilibrium flows of oxygen and nitrogen in nozzles taking into account the excitation of vibrational degrees of freedom," Scientific notes from the N. Ye Zhukovskii Central Institute of Aerohydrodynamics (TsAGI), 8, No. 6 (1977).
7. V. N. Komarov and O. Yu. Polyanskii, "Calculating the temperatures of frozen vibrational degrees of freedom for gas flows in nozzles," Scientific notes from N. Ye. Zhukovskii Central Institute of Aerohydrodynamics (TsAGI), 9, No. 5 (1978).
8. R. Finni, "Dimensionless solutions for flows with vibrational relaxation," Raket. Tekh. Kosmn., 2, No. 2 (1964).
9. S. K. Godunov, A. V. Zabrodin, M. Ya. Invanov, et al., Numerical Solutions for Multidimensional Problems in Gas Dynamics [in Russian], Nauka, Moscow (1976).
10. V. V. Mikhailov and L. Ya. Khaskin, "The discharge of gas from a container placed in a vacuum," Izv. Akad. Nauk SSSR, Mekh. Zhidk. Gaza, No. 1 (1978).
11. V. V. Mikhailov, "The discharge of gas from a restricted volume through a Laval nozzle," Izv. Akad. Nauk SSSR, Mekh. Zhidk. Gaza, No. 2 (1978).
12. V. L. Grigorenko, "Numerical study of shock ignition for supersonic nozzles and a comparison with experimental data," Izv. Akad. Nauk SSSR, Mekh. Zhidk. Gaza, No. 1 (1980).
13. N. V. Stankus, "Numerical study of supersonic nozzles and undersized streams with vibrational relaxation," Preprint 101-83, Institute of Thermal Physics (ITF), Sib. Otd., Akad. Nauk SSSR (1983).
14. L. A. Safronov and V. A. Lebsak, "Non-steady-state processes in electric-arc heaters," Sib. Otd. Akad. Nauk SSSR, No. 3, Issue 1 (1967).
15. L. A. Safronov, "Equations for the transfer processes in electric-arc heaters," Transactions from the N. Ye. Zhukovskii Central Institute of Aerohydrodynamics (TsAGI), No. 1179 (1970).

THE SLOW BURNING CONDITION IN A DUST–GAS MIXTURE

B. M. Smirnov

UDC 536.46

1. Combustion-wave propagation in a gas phase is determined not only by the reaction rate at the maximum temperature of the gas mixture but also by heat transfer through the gas. A rigorous mathematical theory exists [1-5], which relates the wave propagation speed to the parameters of the chemical and thermal processes. In particular, the Arrhenius temperature dependence for the rate constant k, $k \sim \exp(-E_a/T)$, implies that the wave speed u is related to the gas temperature T_m after combustion as follows, where E_a is the activation energy [1, 2]:

$$u \sim \exp(-E_a/2T_m). \tag{1.1}$$

In the burning of a dust–gas mixture, there is an additional process that influences the speed: the emission from the dust particles. If the transverse dimension of the combustion zone is small by comparison with the photon mean free path, the contribution from dust emission to the heat balance is related to the wave speed. The less the speed, the longer the time spent at the maximum temperature and the greater the dust radiation heat loss. In (1.1), the speed is very much dependent on the maximum temperature, so the propagation conditions markedly affect the contribution from emission to the heat balance. This leads to two modes of burning in a dust–gas mixture [6]. In the fast mode, the emission makes a comparatively

Novosibirsk. Translated from Zhurnal Prikladnoi Mekhaniki i Tekhnicheskoi Fiziki, No. 6, pp. 95-103, November-December, 1985. Original article submitted August 23, 1984.